Model-Based Fault Detection Method for Coil Burnout in Solenoid Valves Subjected to Dynamic Thermal Loading

SOO-HO JO[1], BOSEONG SEO[1], HYUNSEOK OH[2], BYENG D. YOUN[1,3,4], AND DONGKI LEE[5]

[1]Department of Mechanical and Aerospace Engineering, Seoul National University, Seoul 08826, South Korea
[2]School of Mechanical Engineering, Gwangju Institute of Science and Technology, Gwangju 61005, South Korea
[3]Institute of Advanced Machines and Design, Seoul National University, Seoul 08826, South Korea
[4]OnePredict Inc., Seoul 08826, South Korea
[5]Data Solution Team, Productivity Research Institute, LG Electronics, Pyeongtaek 17709, South Korea

Corresponding authors: Hyunseok Oh (hsoh@gist.ac.kr) and Byeng D. Youn (bdyoun@snu.ac.kr)

ABSTRACT Solenoid valves are widely used to control fluid flow in various mechanical systems. If the valves do not function properly, the mechanical systems can lose their ability to control the fluid flow. This paper describes a fault detection method that can monitor coil burnout under dynamic thermal loading. The method consists of three steps. First, an equivalent current model of the solenoid valves is derived from Kirchhoff's voltage law. Then, a predictive regression model is developed to describe the relationship between the electric current and the dynamic change of operating temperature of the valves. Finally, a health indicator of solenoid coil burnout is devised in conjunction with the derived model. To demonstrate the validity of the proposed fault detection method, a case study is presented with solenoid valves taken from real braking systems of urban railway vehicles. The case study confirms that the proposed method can detect the coil burnout independent of the operating temperature. We anticipate that the proposed method can be widely applicable to diagnose any electromagnetic actuator of engineered systems as well as solenoid valves in various industrial applications.

INDEX TERMS Electromagnetic actuators, coil burnout, condition-based maintenance, fault detection, regression.

I. INTRODUCTION

Solenoid valves are used to change the path of fluids and to control fluid pressure or flowrate, depending on control voltage magnitudes. Due to their simple operating mechanism, solenoid valves were widely adopted in a variety of industrial applications [1]–[4]. If the valves do not function properly, the system may not perform as intended, thus leading to the potential for serious injuries and/or financial damages. In recent years, to prevent unexpected faults, predictive maintenance strategies have received attention in various industry sectors [5]–[9].

A system's performance depends on its operating environment [10]–[12]. For example, Angadi *et al.* [13] reported that

The associate editor coordinating the review of this manuscript and approving it for publication was Hao Luo.

long operating times and high temperatures could lead to coil overheating, thus accelerating insulation failures or causing an electrical short. Kawashima *et al.* [14] experimentally investigated how air temperature affects the characteristics of the fluid flow rate in the valve. Despite the prior work, it is still challenging to apply fault detection methods in real-world applications where the system performance varies with external temperature. Several types of fluid systems found in real-world applications operate throughout the year and in various climates. In these settings, system temperature changes can result in deviations to the acquired data, thus leading to errors in the results of the fault detection [15]–[17].

With this motivation, this paper proposes a model-based fault detection method that can monitor coil burnout in solenoid valves under dynamic thermal loading. The temperature of the valve itself is determined by two factors; one is the

IEEE *Access*

S.-H. Jo *et al.*: Model-Based Fault Detection Method for Coil Burnout in Solenoid Valves Subjected to Dynamic Thermal Loading

external temperature environment; the other is the Joule heating of the coil during operation. The effects of these factors on the supply current change are modeled. A physics-based regression model is developed from Kirchhoff's voltage law, the resistance-temperature relationship, and Ohm's law. With the proposed regression model, it is found that the health indicator proposed in this study is independent of the temperature by compensating for the supply current change. Thereby, the proposed method can precisely monitor faulty conditions of the valve at any given temperature by comparing the health indicator with a threshold. To the best of authors' knowledge, this research is the first attempt to diagnose solenoid coil burnout under various operating temperatures through the use of a physics-based predictive regression model.

The remainder of this paper is organized as follows. Section II provides a brief review of fault modes and detection methods for solenoid valves. Section III presents the proposed model-based fault detection method for detecting coil burnout. As a case study, Section IV demonstrates the experimental setup and procedure to diagnose service-braking valves used in braking systems of urban railway vehicles. The validation of the proposed method is covered in Section V. This paper concludes with future works in Section VI.

II. A REVIEW OF FAULT DETECTION FOR SOLENOID VALVES

This section provides a literature review of fault detection of solenoid valves. Section A presents the failure mode, mechanism, and effects analysis of valves. Section B describes the state-of-the-art-fault detection methods for solenoid valves.

A. FAILURE MODE, MECHANISM, AND EFFECTS ANALYSIS

From maintenance histories provided by Seo *et al.* [18], the dominant failure modes were identified as (i) solenoid coil burnout, (ii) rubber seat damage, and (iii) debris accumulation. In Table 1, the causes, effects, and related condition monitoring signals are summarized in accordance with individual fault modes.

First, solenoid coil burnout can occur when the coil is corroded or the wire coating is partially peeled off. These factors result in changing the magnitudes of both the effective resistance and the supply current. Therefore, the coil burnout triggers errors in feedback systems; excessive or deficient current prevents air from being supplied to other components.

Second, the magnetized armature and the valve bar move up and down repeatedly whenever the valve is on and off, thereby applying fatigue loads to the top surface of the rubber seat. Repeated contact forces make a line hole on it and lead to a leakage of the input pressure due to an oscillation of the rubber seat. Therefore, it confuses the feedback control system.

Last, metallic debris, created by the friction between metals in other systems, can be flowed inside the valve. Then, the debris can accumulate on the top surface of the rubber seat, resulting in continuous leakage of the output pressure.

It thus leads to providing other components with insufficient pressure.

B. FAULT DETECTION METHOD FOR SOLENOID VALVES

Existing fault detection methods often use vibration signals. Tsai and Tseng [19] developed a dynamic model-based method to detect surface damages on the valve bar and seat for electronic diesel fuel injection systems. After updating model parameters, representing surface damage characteristics, from vibration signals, artificial neural networks were used to classify normal and faulty conditions. Guo *et al.* [20] proposed a data-driven method to detect solenoid coil degradation in brake systems. A fault was detected when the acceleration, which was denoised by a wavelet algorithm, was less than a threshold. Despite the high detection sensitivity of the vibration signal-based methods, the installation of invasive sensors in target valves can be a burden in real-world applications.

On the other hand, the noninvasiveness of fault detection methods based on current signals can be a considerable advantage over methods based on vibration signals. Börner *et al.* [21] developed a model-based method to detect abnormal behaviors of the armature. Health conditions were evaluated by calculating the residual between the mechanical position of the armature from the electromagnetic model and the reconstructed model using electric signals in faulty valves. Guo *et al.* [22] demonstrated a data-driven method to classify failure modes of valves. Current signal characteristics for six failure modes were extracted by using empirical mode decomposition. Classification results using the proposed multi-kernel support vector machine showed the high accuracy of 98.9 %.

Previous studies are limited in that experiments were performed at a fixed temperature. Dynamic changes of ambient temperature can make physical parameters of valves deviate from nominal values. The effect of dynamic changes should be thus incorporated into fault detection models. Besides, according to the experts in the field of valve systems, the coil burnout is the most dominant among fault modes. This motivates to develop a model-based fault detection method that can capture the coil burnout in solenoid valves under various operating temperatures.

The contributions of this study can be summarized into three aspects. First, a new health indicator is proposed. Unlike the previous study [18], it can be calculated by only electrical current without pressure signals. It is more efficient in practical applications. Second, this method considers not only the effect of Joule heating during the operation but also that during external temperature changes that arise from the valve's environment. In [18], only the effect of Joule heating is taken into account. Last, the proposed regression model shows the severity of coil degradation quantitatively.

III. SIMULATION MODEL

This section describes the simulation model used to detect the burnout of the solenoid valve coils. The effect of dynamic

S.-H. Jo *et al.*: Model-Based Fault Detection Method for Coil Burnout in Solenoid Valves Subjected to Dynamic Thermal Loading

IEEE *Access*

TABLE 1. Failure mode, mechanism, and effect analysis of the solenoid Valve.

Part	Failure mode	Mechanism	Effect	Condition monitoring signals
Solenoid coil	Coil burnout	Corrosion	Excessive current	Supply current
Rubber seat	Damage	Fatigue	Air leakage	Input pressure
	Debris accumulation	Wear	Air leakage	Output pressure

Current and Temperature Signals

| Equivalent circuit model | Step 1: Calculate the maximum supply current I_{max} |

| Predictive regression model (Current-Temperature) | Step 2: Calculate coefficients of the regression model |

$$K\alpha = \frac{V_{ctrl} R_{int}(T_0) \alpha}{\left(R_{ext}(T_0) + R_{int}(T_0)\right)^2}$$

Step 3: Compensate the reduction of the maximum supply current I_{max}

Step 4: Calculate the health indicator I_{HI}

$$I_{HI} = I_{max}(t) + K\alpha\left(T(t) - T_0\right)$$

> Threshold

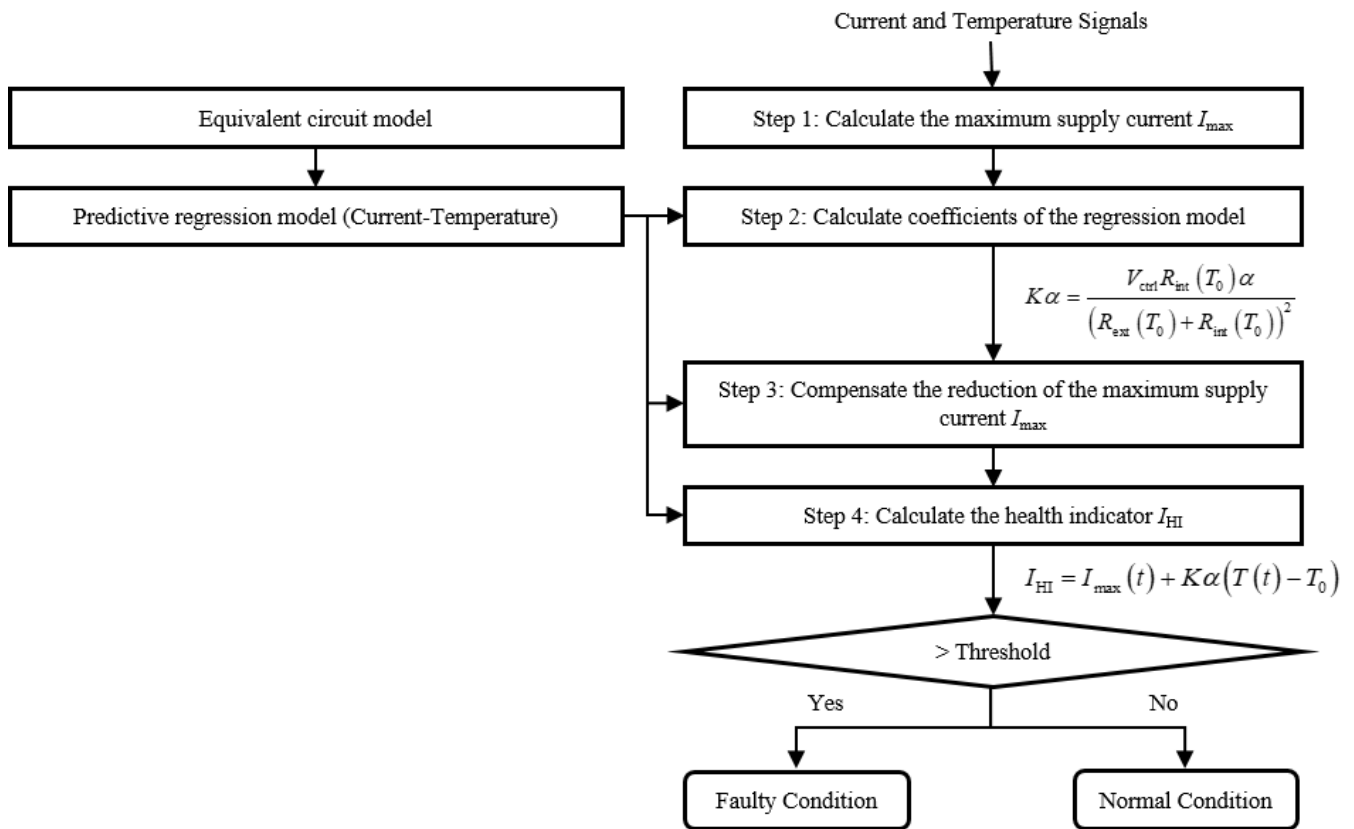Yes — Faulty Condition

No — Normal Condition

FIGURE 1. A flowchart of the proposed model-based fault detection method for coil burnout in solenoid valves subjected to dynamic thermal loading.

thermal loads on the supply current to the coils is considered in the simulation model.

The overall procedures to detect the coil burnout using the simulation model are shown in Fig. 1. At first, a predictive regression model between the supply current and temperature is quantitatively derived from equivalent circuit modeling and effects of temperature on electrical resistivity. As shown in Fig. 1, with the inputs of current and temperature signals, a health indicator determines whether the valves are in faulty conditions (or not) by comparing with a threshold. Additional details are provided in the following subsections.

Section A presents an equivalent circuit model to derive the explicit form of the supply current. Section B describes the effect of the thermal loads on the supply current. The mathematical relation between the coil temperature and the supply current is derived. In conjunction with the derived

model and current-temperature relation, Section C proposes a health indicator for the solenoid coil burnout.

A. EQUIVALENT CIRCUIT MODELING OF A SOLENOID VALVE

This subsection presents the equivalent circuit model of the valve to describe the relation between the control voltage and the supply current. Fig. 2 presents a circuit diagram of the coil that consists of the inductance and internal electrical resistance of the coil itself, and the external electrical resistance that is connected to the circuits. The mechanical positions of the subcomponents were elucidated by multiphysics mechanisms; electromagnetic, fluidic, and dynamic forces were coupled [23]. Likewise, the voltage-current equation was derived from the Kirchhoff's voltage law, that allows consideration of the effects of mechanical positions on the
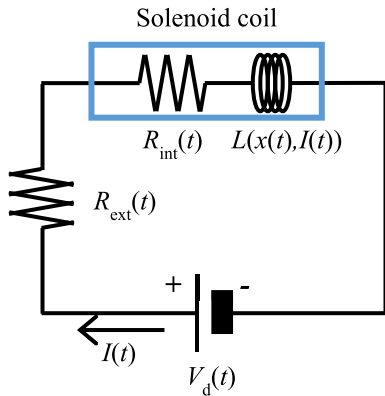
IEEE *Access*

S.-H. Jo *et al.*: Model-Based Fault Detection Method for Coil Burnout in Solenoid Valves Subjected to Dynamic Thermal Loading

FIGURE 2. A circuit diagram of the coil in a solenoid valve.

potential difference [24]:

$$
\begin{aligned}
V_d(t) = {} & (R_{ext}(T(t)) + R_{int}(T(t)))I(t) \\
& + L(x(t), I(t))\frac{dI(t)}{dt} + E(x(t), I(t))\frac{dx(t)}{dt}
\end{aligned} \quad (1)
$$

where $V_d(t)$ and $I(t)$ are the control voltage and supply current, respectively; $R_{ext}(T(t))$ and $R_{int}(T(t))$ represent the external and internal electrical resistances as a function of the temperature $T(t)$ of the solenoid coils; $L(x(t), I(t))$ is the incremental inductance of the coil; $E(x(t), I(t))$ is the motional electromotive force; and $x(t)$ is the distance between the center of the armature and the coil.

The control voltage is the summation of (i) the potential difference due to the resistances $R_{ext}(T(t))$ and $R_{int}(T(t))$, (ii) the induced voltage due to the incremental inductance $L(x(t), I(t))$, and (iii) the motional electromotive force due to the movement of the armature. Among three terms, the third one can be considered insignificant, since the voltage induced by the motional electromotive force is less than 2% of the control voltage $V_d(t)$, under the assumption that the velocity of the armature is negligible [25]. Therefore, (1) can be rewritten as:

$$
\begin{aligned}
V_d(t) = {} & (R_{ext}(T(t)) + R_{int}(T(t)))I(t) \\
& + L(x(t), I(t))\frac{dI(t)}{dt}
\end{aligned} \quad (2)
$$

The incremental inductance $L(x(t), I(t))$ is the differentiation of the flux leakage $\lambda(x(t), I(t))$ with respect to the supply current $I(t)$, as shown in (3).

$$
L(x(t), I(t)) = \frac{\partial \lambda(x(t), I(t))}{\partial I(t)} \quad (3)
$$

The flux leakage $\lambda(x(t), I(t))$ can be expressed as the multiplication of the turns of the coil N and magnetic flux $\varphi(x(t), I(t))$. The magnetic flux is the surface integral of the normal component of the magnetic field $B(x(t), I(t))$ through the cross-section S of the coil [26].

$$
\lambda(x(t), I(t)) = N \oint_S B(x(t), I(t)) \cdot dS \quad (4)
$$

When the radius R_{coil} of the coil is comparable to the length l_{coil} of it, the magnetic field $B(x(t), I(t))$ can be derived from Biot-Savart's law as

$$
\begin{aligned}
& B(x(t), I(t)) \\
& = \frac{\mu_0 N I(t)}{2 l_{coil}} \left[-\frac{x(t) - \dfrac{l_{coil}}{2}}{\left(\left(x(t) - \dfrac{l_{coil}}{2}\right)^2 + R_{coil}^2 \right)^{1/2}} \right. \\
& \qquad\qquad \left. + \frac{x(t) + \dfrac{l_{coil}}{2}}{\left(\left(x(t) + \dfrac{l_{coil}}{2}\right)^2 + R_{coil}^2 \right)^{1/2}} \right]
\end{aligned} \quad (5)
$$

where μ_0 is known as the permeability in a vacuum [27]. Under the assumptions that the constant voltage is applied as a reference voltage and the mechanical position $x(t)$ of the armature reaches a steady-state, a constant magnetic field $B(x(t), I(t))$ results in the flux leakage remaining constant in (4); furthermore, the incremental inductance $L(x(t), I(t))$ is also constant as a reference inductance in (3). To avoid potential confusion, the incremental inductance $L(x(t), I(t))$ and control voltage $V_d(t)$ are denoted as L_{ref} and V_{ctrl}, respectively. From (2), the control voltage can be rewritten as

$$
V_{ctrl} = (R_{ext}(T(t)) + R_{int}(T(t))) I(t) + L_{ref}\frac{dI(t)}{dt} \quad (6)
$$

The original equation (1), reduced to a first-order ordinary linear differential equation with constant coefficients, is shown in (6). The exact solution of (6) can be obtained using Laplace transform and inverse Laplace transform as

$$
I(t) = \frac{V_{ctrl}}{R_{ext}(T(t)) + R_{int}(T(t))} e^{1 - \frac{R_{ext}(T(t)) + R_{int}(T(t))}{L_{ref}}t} \quad (7)
$$

The inverse of the coefficient of the time t is a so-called time constant. In the case of the solenoid valve under consideration, the internal electrical resistance $R_{int}(T(t))$ is several hundreds of Ω, while the reference inductance L_{ref} is several hundreds of mH. Then, the time constant has an order of 10^{-3} second. Therefore, the supply current $I(t)$ reaches a steady-state in an order of milli-seconds. Based on the modeling assumptions, the supply current $I(t)$ can be regarded as the ratio of the control voltage V_{ctrl} to the summation of the external and internal electrical resistances $R_{ext}(T(t))$ and $R_{int}(T(t))$ as

$$
I(t) = \frac{V_{ctrl}}{R_{ext}(T(t)) + R_{int}(T(t))} \quad (8)
$$

When the electrical resistances $R_{ext}(T(t))$ and $R_{int}(T(t))$ subjected to thermal loading deviate from nominal values in a single cycle, the electrical resistances cannot be regarded as constants. However, the electrical resistance can be assumed to be constant when the thermal loads are negligible. To this end, the external and internal electrical resistances $R_{ext}(T(t))$
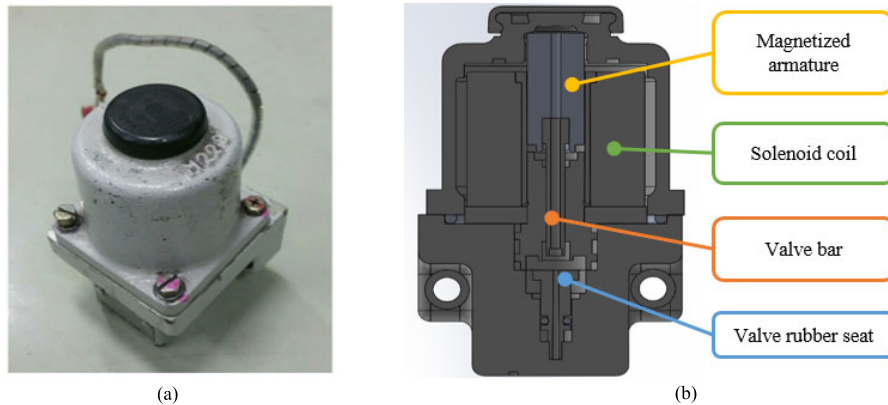
S.-H. Jo *et al.*: Model-Based Fault Detection Method for Coil Burnout in Solenoid Valves Subjected to Dynamic Thermal Loading

IEEE *Access*

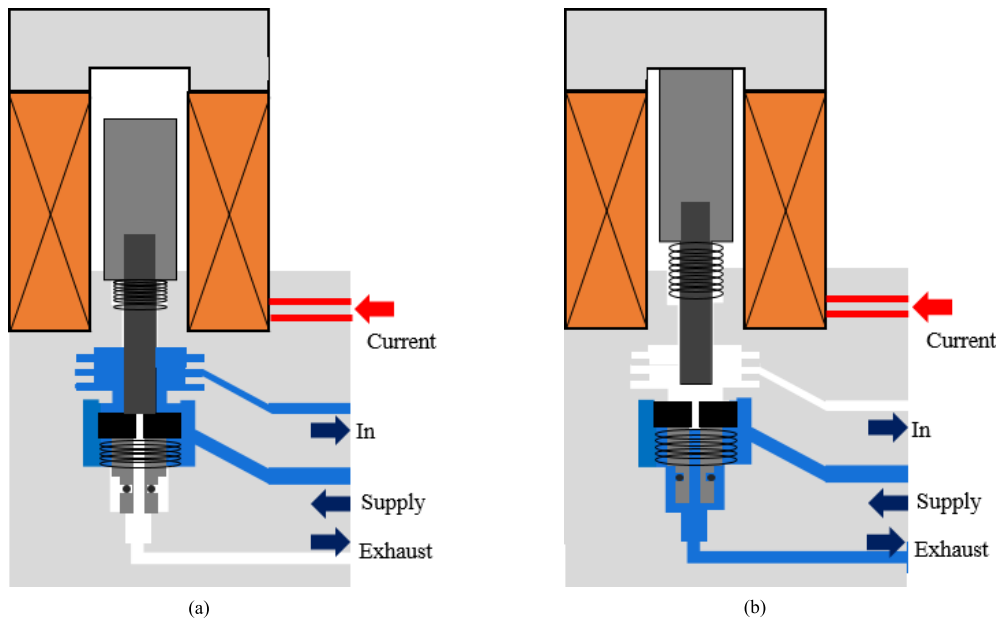**FIGURE 3.** Service braking valve configuration: (a) external view and (b) cross sectional view.

FIGURE 4. A schematic view of a service braking valve: (a) supply mode and (b) exhaust mode.

and $R_{int}(T(t))$ are denoted as $R_{ext}(T_0)$ and $R_{int}(T_0)$ as

$$I(t) = \frac{V_{ctrl}}{R_{ext}(T_0) + R_{int}(T_0)} \quad (9)$$

where T_0 is the initial temperature of the solenoid coils. The initial temperature at $t = 0$ is called a reference temperature in this study.

B. EFFECT OF TEMPERATURE ON SOLENOID COIL RESISTIVITY

The equivalent circuit model in previous section can be used when the amount of thermal load to the solenoid coils is not significant. For example, when solenoid valves operate in a single cycle, the increase of solenoid coil temperature will be negligible. However, when solenoid valves operate continuously, the increase of the solenoid coil temperature by Joule heating cannot be ignored. The Joule heating can increase solenoid coil resistivity, thereby increasing the resistances that are functions of resistivity, cross-section, and length of
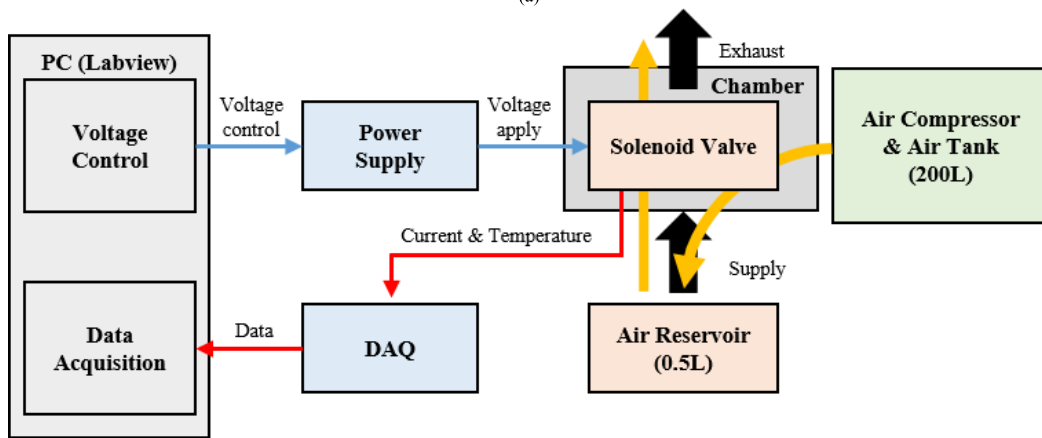
the conducting wires. The prior assumption of constant temperature does not hold any more. Thus, the effect of thermal loads on solenoid coils should be incorporated.

In (9), the supply current is inversely proportional to the summation of the electrical resistances of the coil so that the supply current will decrease with the increase of the temperature. The supply current reduction with respect to the temperature (or time) not only lowers the reliability of the fault detection method but also results in a wrong decision about the health conditions. Therefore, it is required to quantify the degree of the supply current reduction and compensate for it.

It is assumed that the external electrical resistance is exposed to the external temperature environments and also that the Joule heating of the coil does not affect the temperature of the external electrical resistance. The initial external and internal electrical resistances are denoted as $R_{ext}(T_0)$ and $R_{int}(T_0)$, respectively. These initial resistances are called reference resistances in this study. It is known that the internal resistance change is linear to the temperature change $T(t)$-T_0

IEEE Access

S.-H. Jo *et al.*: Model-Based Fault Detection Method for Coil Burnout in Solenoid Valves Subjected to Dynamic Thermal Loading

FIGURE 5. Testbed setup: (a) testbed configuration and (b) design of experiment.

with the coefficient $\alpha R_{\text{int}}(T_0)$, as

$$R_{\text{int}}(T(t)) = R_{\text{int}}(T_0) + \alpha R_{\text{int}}(T_0)(T(t) - T_0) \quad (10)$$

where $T(t)$ is the ambient temperature at time t, and the reference temperature T_0 is identical to the initial external temperature. By substituting (10) into (9), the supply current change can be expressed as

$$I_0 - I(t) = \frac{V_{\text{ctrl}}}{R_{\text{ext}}(T_0) + R_{\text{int}}(T_0)}$$
$$- \frac{V_{\text{ctrl}}}{R_{\text{ext}}(T_0) + R_{\text{int}}(T_0)(1 + \alpha(T(t) - T_0))} \quad (11)$$

where I_0 is the initial supply current of the coil. For a conductor material, the temperature coefficient of the resistivity α is the constant in several ones of 1/mK [27]. Equation (11) can be thus rewritten as follows using the Taylor series with a negligible error:

$$I_0 - I(t) = \frac{V_{\text{ctrl}} R_{\text{int}}(T_0) \alpha}{(R_{\text{ext}}(T_0) + R_{\text{int}}(T_0))^2}(T(t) - T_0)$$
$$= K\alpha(T(t) - T_0) \quad (12)$$

where K is the proportional constant. The degree of supply current reduction over time is derived mathematically. This indicates that the supply current change has linear relationship with the temperature change.

Rearranging (12) with respect to the time t,

$$I_0 = I(t) + K\alpha(T(t) - T_0) \quad (13)$$

Equation (13) provides a method that can estimate the initial supply current of the coil over time. For example, at $t = 0$, I_0 can be measured without (13), while at $t = 10$, I_0 can be estimated from (13) with the measurement of $I(t = 10)$ and $T(t = 10)$. The initial supply current I_0 of the coil can be calculated at any time of interest. This gives an idea that I_0 in (13) can be a health indicator independent of time.
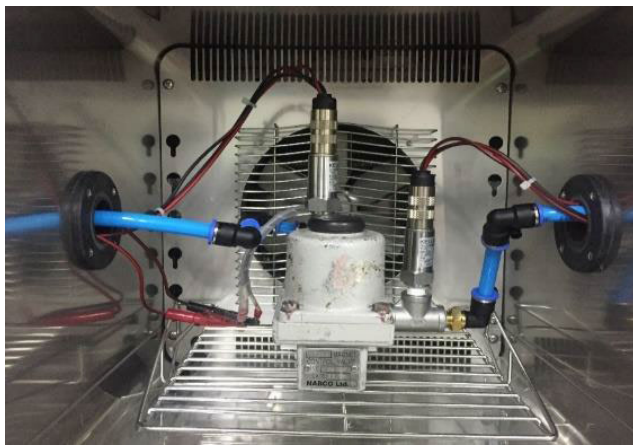
C. PROPOSED HEALTH INDICATOR I_{HI}

The proposed health indicator, denoted as I_{HI}, is expressed as

$$I_{\text{HI}} = I_{\text{rep}}(t) + K\alpha(T(t) - T_0) \quad (14)$$

where I_{rep} is the representative supply current at time t. As shown in Fig. 7 (a), the supply current value changes over time within a single cycle. Therefore, it is needed to determine the representative supply current value at each cycle. For

S.-H. Jo *et al.*: Model-Based Fault Detection Method for Coil Burnout in Solenoid Valves Subjected to Dynamic Thermal Loading

IEEE *Access*

TABLE 2. Standard for external temperature environment (KS R 9156).

Classification		Low-temperature test		High-temperature test	
		Operation guarantee temperature (°C)	Performance guarantee temperature (°C)	Operation guarantee temperature (°C)	Performance guarantee temperature (°C)
Type 1	Type A	0	5	55	40
	Type B	-10	-10		
	Type C			60	55
Type 2	Type A		5	55	40
	Type B	-20	-10		
	Type C			60	55

FIGURE 6. A solenoid valve deployed inside the temperature and humidity chamber.

example, $I_{rep}(t)$ can be the maximum value (i.e., I_{max}) of the supply current at the cycle which the time corresponds to.

The proposed health index eliminates the effect of temperature change on the representative supply current at time t. Therefore, the proposed health index is independent of temperature change, i.e., temperature-independent health indicator for coil burnout in solenoid valves.

When solenoid coils are degraded, the electrical resistance of degraded coils is smaller than that of normal coils. This leads that the health indicator will deviate from the nominal value that is calculated when the solenoid coils are in a normal condition. Therefore, if a health indicator I_{HI} of a solenoid valve exceeds a threshold $I_{HI,th}$, the valve can be considered to be in faulty conditions. The threshold $I_{HI,th}$ is defined using the first rule in statistical process control charts (i.e., Nelson rule) as follows:

$$I_{HI,\,th} = \mu_{HI} + 3\sigma_{HI} \qquad (15)$$

where μ_{HI} and σ_{HI} stand for the mean and the standard deviation of health indicators I_{HI} of new and/or normal valves, respectively. A failure occurs if the health indicator I_{HI} exceeds three standard deviations from I_{HI} of new and/or normal valves.

The proposed health indicator I_{HI} is different from the supply current at 10% output pressure in the previous study [18]. The proposed health indicator I_{HI} can be calculated with only electrical current waveforms that flow through the solenoid coil. The proposed health indicator I_{HI} does not require the measurement of outlet pressure that was required in [18].

IV. EXPERIMENT
This section presents the experimental setup of the research, which examined solenoid valves under various thermal loading conditions. The specimens, called service braking valves, are real solenoid valves taken from the braking systems of urban railway vehicles operated by the Seoul Metropolitan Rapid Transit Corporation. Six specimens were used in the study, including: (i) four used and normally functioning valves ("normal valves"), (ii) one new valve, and (iii) one faulty valve. The external view of a service braking valve is shown in Fig. 3 (a) while the cross-sectional view of the valve is illustrated in Fig. 3 (b). The key components of a service braking valve include solenoid coils, two springs, a magnetized armature, a valve bar, and a rubber valve seat. The volume of the valve is less than 65 mm × 70 mm × 105 mm and a cover encloses the inner space to prevent air leakage.

In the field, the service braking valves are controlled to offer four operating modes: (i) supply, (ii) supply standby, (iii) exhaust, and (iv) exhaust standby. The operating modes can be selected by controlling the input voltage. Under the supply and exhaust modes, as depicted in Fig. 4, the air flows in and out, respectively. Under the supply mode and the supply stand-by mode, an electromagnetic force actuates the armature and valve bar in a downward direction. The armature, valve bar and the valve seat come into contact; thus, they can be regarded as one object. This movement gives rise to the inflow of air. On the other hand, in the exhaust mode and exhaust standby mode, a small amount of voltage is supplied to allow a so-called air gap. Since the armature and valve bar put distance from the valve seat they move as one object. The air gap gives rise to the outflow of air.

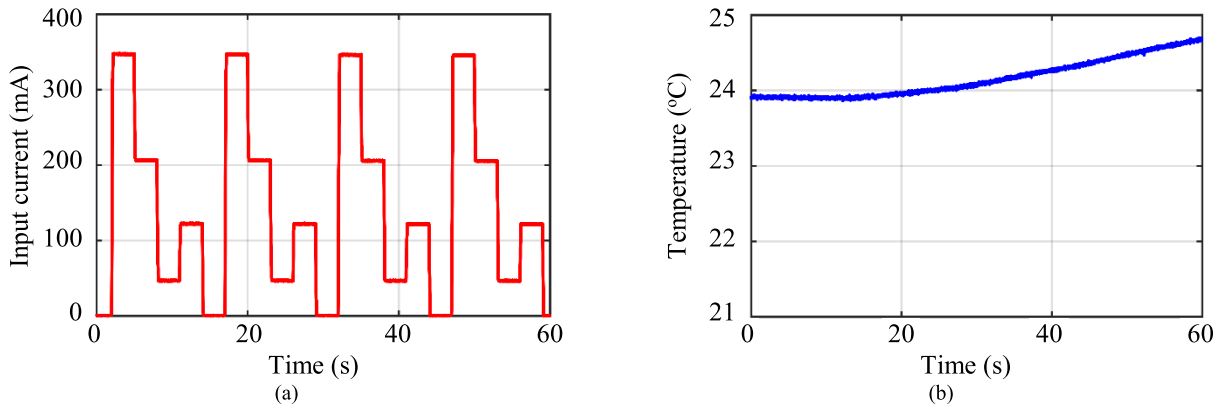The braking systems in an urban railway are operated throughout the year; thus, they are exposed to different

FIGURE 7. Input current and temperature profiles for first four cycles at room temperature: (a) input current and (b) temperature.
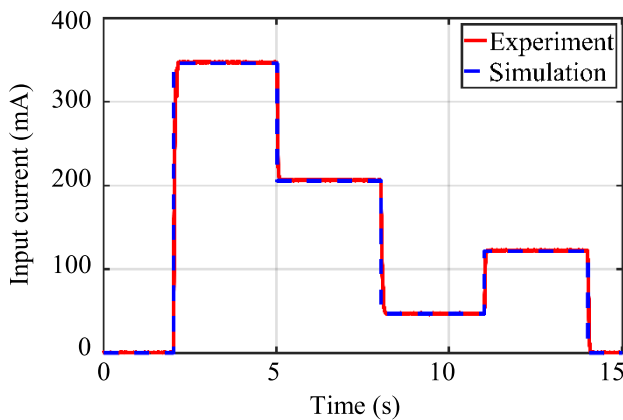

FIGURE 8. Supply current profile obtained from both the simulation and experiment.
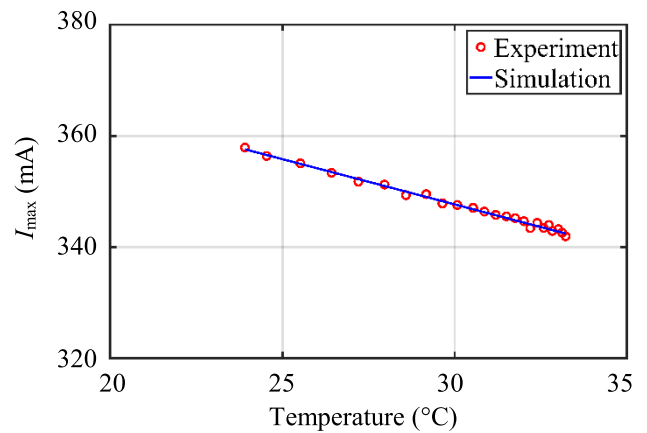

FIGURE 9. Relationship between maximum supply current I_{max} and temperature in both the simulation and experiment.

temperatures (e.g., throughout the four seasons in the Republic of Korea). KS R 9156 is used to define the external temperature environments to test electronic devices used in railway vehicles. As shown in Table 2, Types 1 and 2 correspond to the cases in which the minimum value of the storage temperature of the device is -10 °C and -25 °C, respectively. Types A, B, and C indicate the indoor device, outdoor device, and outdoor device housed in another device, respectively. The service braking valve is classified as Type 1 and Type C. Since this study examines the performance degradation during operation, the external temperature of the valves was set to be -10 °C and 55 °C in the low- and high-temperature tests, respectively. In both tests, the external temperature should increase (or decease) to the performance guarantee temperature until reaching an equilibrium state within 3 °C of the temperature, while maintaining this equilibrium state for one hour. During the temperature regulation process, the room temperature in the laboratory was fixed to be 24 °C to avoid the possibility of the external temperature affecting the control performance.

The testbed configuration and design of experiment are presented in Figs. 5 (a) and (b), respectively. To control the operating performance of the valve, the software LabVIEW2008 was used. A voltage-control algorithm in

LabVIEW2008 applied the voltage to the solenoid coil through a power supply (BK Precision, 1710A). The solenoid coil was deployed inside the temperature and humidity chamber (ESPEC Corp., SH-241); this chamber controlled the dynamic thermal loading, as shown in Fig. 6. An air compressor (ACOM, OS100) provided air into the air receiver tank (GA Korea, GAT-0020). In the supply mode, the compressed air was supplied to the solenoid valve and the air reservoir. In the exhaust mode, the stored air in the air reservoir was released. Throughout this process, a data acquisition device (National Instruments, USB-6009) put digital signals controlled by LabVIEW into the power supply and stored the measured data. The air receiver tank, reservoir, and chamber were used due to challenges in mimicking the actual operating environments and components of the real-world braking system.

The measured data included the supply current from an attached terminal on the external electrical resistance of 1 Ω connected to the coil and temperature from thermocouples (MiraeTech, MR-2320) attached to the surface of the coil. The reference resistances of the solenoid coils were measured using LCR Meters (Keysight Technologies, E4980A). A voltage-control algorithm was developed; 37 V, 22 V,
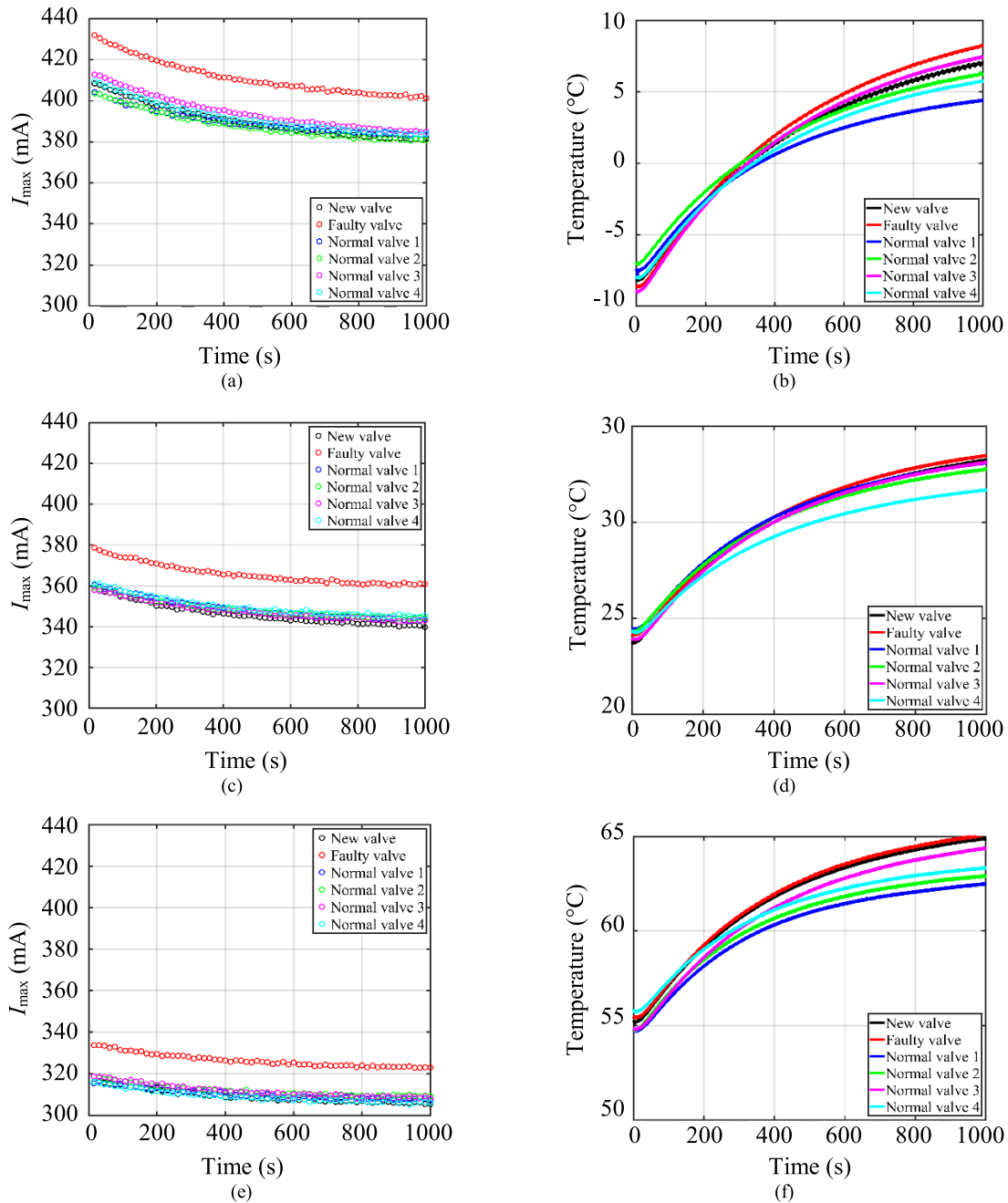
S.-H. Jo *et al.*: Model-Based Fault Detection Method for Coil Burnout in Solenoid Valves Subjected to Dynamic Thermal Loading

IEEE *Access*

FIGURE 10. The maximum input current I_{max} and temperature profile in the time domain under different external temperature environments: (a) maximum supply current I_{max} at low temperature (-10 °C); (b) temperature profile at low temperature (-10 °C); (c) maximum supply current I_{max} at room temperature (24 °C); (d) temperature profile at room temperature (24 °C); (e) maximum supply current I_{max} at high temperature (55 °C); and (f) temperature profile at high temperature (55 °C).

5 V, and 13 V were applied in the supply, supply standby, exhaust, and exhaust standby modes, respectively. Each mode was tested for three seconds. 70 cycles were taken to complete one experiment. As a representative sample of one normal valve, the supply current and temperature profiles for the first four cycles at room temperature are shown in Figs. 7 (a) and (b), respectively. As shown in Fig. 7 (a), a relatively high current was obtained due to the high voltage in the supply and supply standby modes. In addition,

temperature increases were observed due to Joule heating as shown in Fig. 7 (b).

V. RESULT AND DISCUSSION

This section describes the results and discusses the effectiveness of the proposed method for solenoid coil burnout. Simulation results are compared with experiment results for the room temperature scenario. Supply current profiles from simulation and experiment are compared for the first cycle at
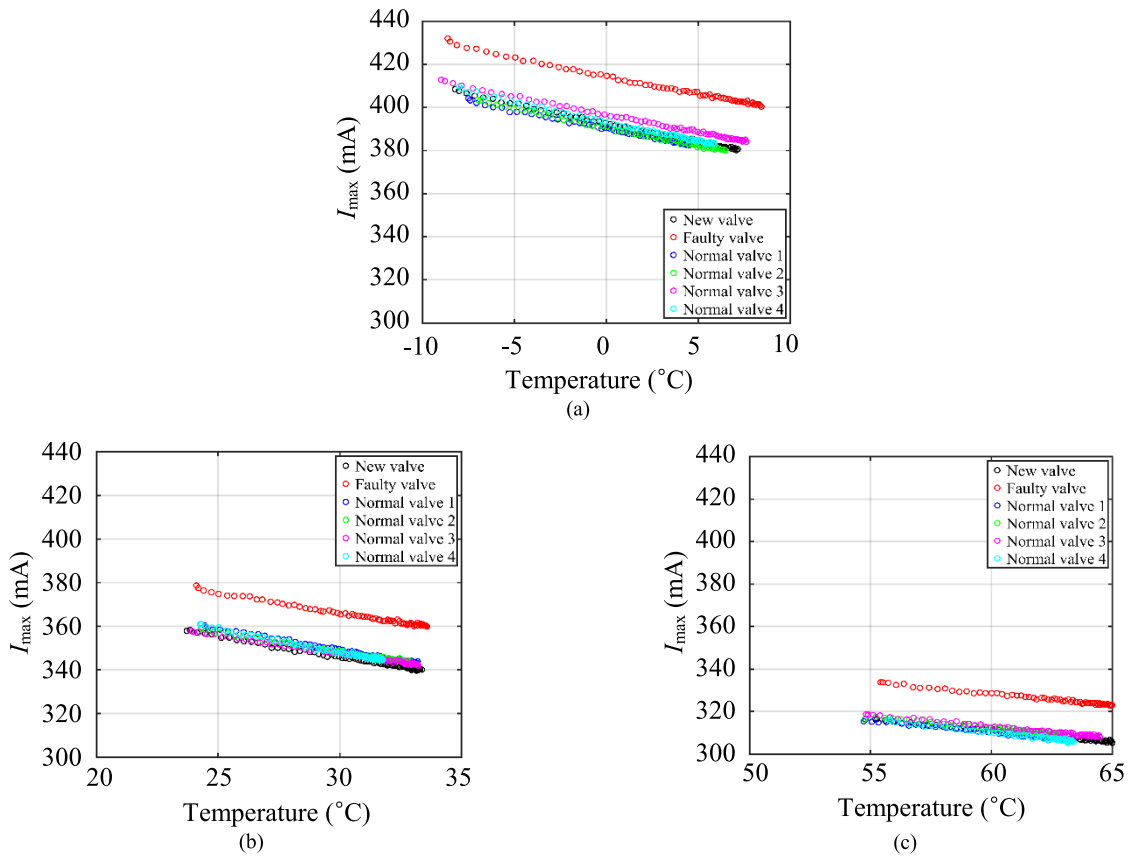
IEEE Access

S.-H. Jo et al.: Model-Based Fault Detection Method for Coil Burnout in Solenoid Valves Subjected to Dynamic Thermal Loading

FIGURE 11. Relationship between maximum supply current I_{max} and temperature under different external temperature environments: (a) low temperature (-10 °C); (b) room temperature (24 °C); and (c) high temperature (55 °C).

room temperature. Under the assumption that the temperature change was not significant during a single cycle, the initial temperature of the valve was set to be at the room temperature of 24 °C. The supply current profile in the numerical simulation was obtained from (9). As shown in Fig. 8, it was observed that two profiles overlap with negligible gap from visual inspection.

During 70 cycles of solenoid valve operation, the maximum supply current I_{max} was extracted in the supply mode at each cycle. It should be noted that the health indicator I_{HI} stands for the maximum supply current after compensating for the degree of supply current reduction by using (12); on the other hand, I_{max} stands for those without the compensation task. The relationship between the maximum supply current I_{max} and temperature of the valve is depicted in Fig. 9. Blue solid and red dotted lines indicate results of the numerical simulation and experiments, respectively. Simulation results were obtained from (12). It is worth noting that the results from the numerical simulation are in good agreement with those from the experiments. This implies that the equivalent circuit modeling with the assumptions and the developed regression model can demonstrate the operating performance of the valve.

The same procedures were repeated for another valves under different temperature environments. The trends of

maximum supply current I_{max} at low, room, and high temperatures are shown in Figs. 10 (a), (c), and (e), respectively; the x-axis indicates the number (or order) of obtaining the maximum supply current I_{max} per three cycles. The temperature in the time domain at low, room, and high temperatures is shown in Figs. 10 (b), (d), and (f), respectively. Lines or circles colored with blue, black, red, green, magenta, and cyan indicate the quantities (i.e., maximum supply current I_{max} and temperature) for the one new, one faulty, and four normal valves, respectively.

There are three key points from this work. First, when investigating the absolute values of maximum supply current I_{max} in Figs. 10 (a), (c), and (e), the maximum supply current I_{max}, satisfies the modeling assumptions in Section III, and presents indicators for the faulty valve that are higher than the others in all cycles. Moreover, from the perspective of the trend in terms of cycles, the maximum supply current I_{max} decreases due to the Joule heating as the valve keeps working in each temperature environment. Last, when examining the value of initial health indicator I_{HI} at the first cycle, it is different in the three different temperature environments that were examined. For example, when the external temperature goes down to the low temperature of -10 °C, the overall resistance increases and the supply current decreases. This shows that the experimental results are in good agreement
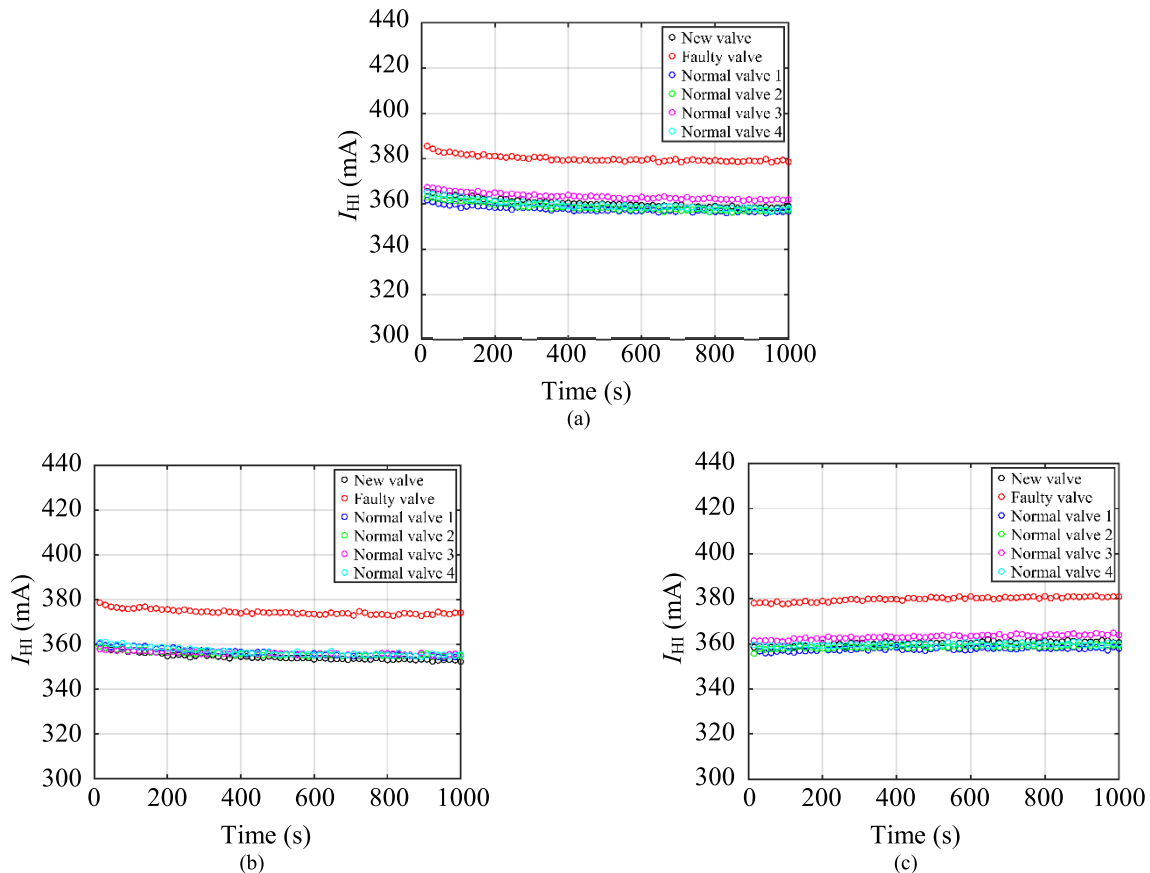
S.-H. Jo *et al.*: Model-Based Fault Detection Method for Coil Burnout in Solenoid Valves Subjected to Dynamic Thermal Loading

IEEE *Access*

FIGURE 12. Comparison of the compensated health indicator I_{HI} under different external temperature environments at: (a) low temperature (-10 °C); (b) room temperature (24 °C); and (c) high temperature (55 °C).

TABLE 3. Coefficient $K\alpha$ of the temperature to the maximum supply current I_{max} (mA/°C).

Valve Type	New	Faulty	Normal 1	Normal 2	Normal 3	Normal 4
Measurement	1.3213	1.4054	1.3368	1.3342	1.3342	1.3355
Curve Fitting	1.3427	1.4167	1.3331	1.3166	1.3380	1.3380

with our physical interpretation. This supports the need to develop a method for detecting solenoid coil burnout under various operating temperatures.

The maximum supply current I_{max} in terms of the temperature are presented in Figs. 11 (a), (b), and (c) at low, room, and high temperature conditions, respectively. The maximum supply current I_{max} linearly decreases for the temperature. Therefore, (12) enables compensation for the degree of the maximum supply current I_{max} reduction as a standard of the initial value of the maximum supply current I_{max}. When performing the compensation tasks in each external temperature environment, it can be found that the health indicator I_{HI} is independent of the temperature change that is caused by the Joule heating. However, it can be difficult to standardize an absolute fault criterion, since the compensated values rely on the external temperature environments. It is thus required to

perform compensation tasks for the overall operating temperature conditions.

This paper attempted to develop a fault detection method that uses only the data types being acquired in industrial fields, without the need for any additional sensors. To use (12), the values of internal resistances are required; however, in real-world settings, no sensor can be available to measure these resistances [28]. In this case, it is necessary to perform curve fitting using the proposed linear regression model of (12). In the case of the constant term, the first health indicator I_{HI} at room temperature can be considered. Table 3 summarizes the coefficients of the linear model obtained from measuring the resistances and those estimated from curve fitting. It was found that the coefficients obtained from the proposed linear regression model are in good agreement with those estimated from curve fitting for all six valves. This
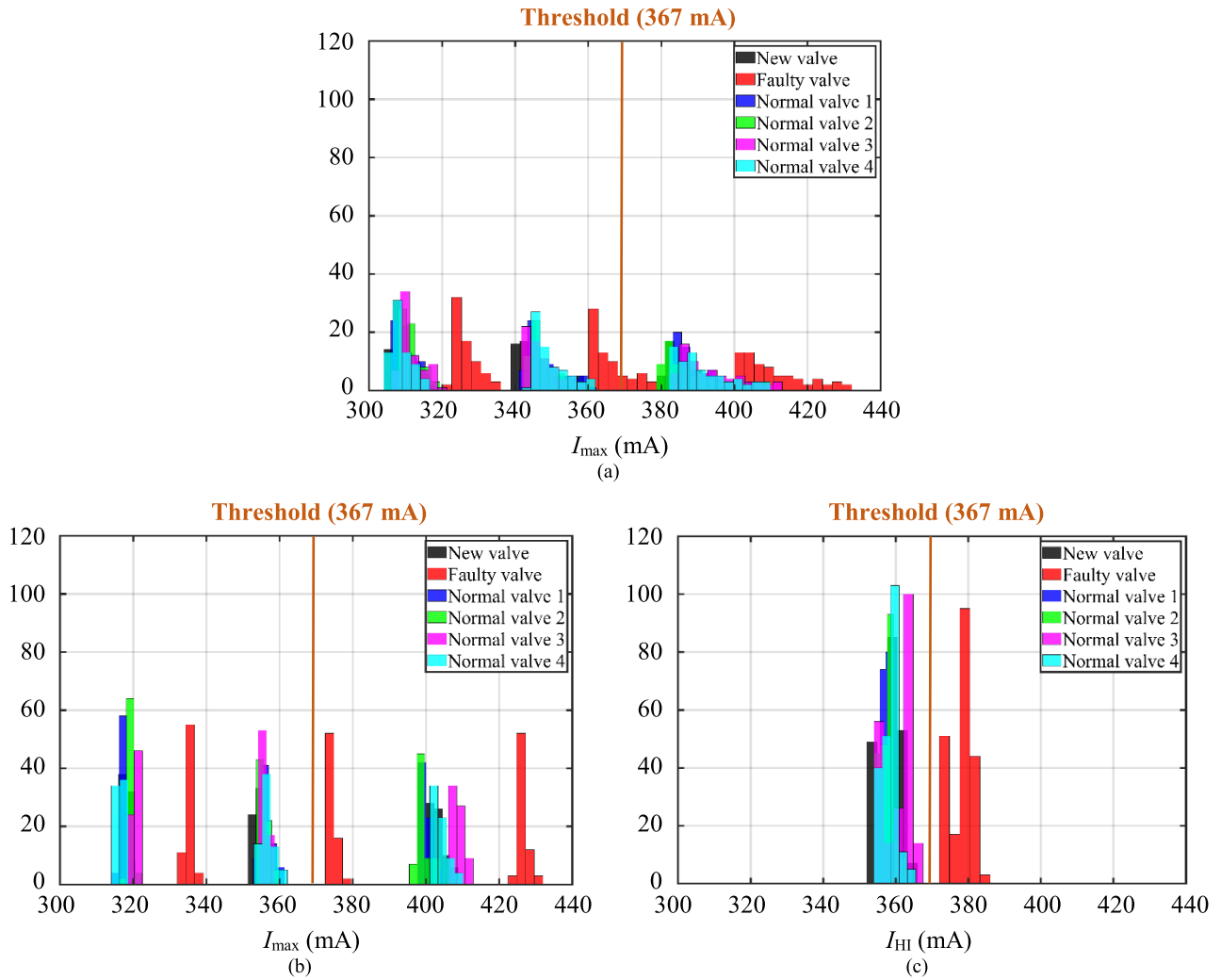
FIGURE 13. Fault detection results of solenoid coil burnout for six service braking valves subjected to dynamic thermal loading: (a) maximum supply current I_{max} without compensation; (b) compensated maximum supply current I_{max} considering only the Joule heating of the coils under each temperature environment; and (c) proposed health indicator I_{HI}.

indicates that the curve fitting in the experiments represents the physical domain knowledge, not signal processing. Therefore, if the internal resistances are unknown for an arbitrary time in the field, curve fitting can still enable solenoid coil burnout detection. The compensation results are presented in Figs. 12 (a), (b), and (c) under the low, room, and high temperature conditions, respectively. As a result, the value of the health indicator I_{HI} for each valve is almost identical, independent of external temperature environments and Joule heating of the valve itself.

Figs. 13 (a), (b), and (c) show histograms for the following three cases, respectively: (i) maximum supply current I_{max} without any compensation task, (ii) compensated maximum supply current I_{max} considering only the Joule heating of the coils under each external temperature environment, as the previous study [18] did, and (iii) the proposed health indicator I_{HI}. In Figs. 13 (a) and (b), due to temperature effects, it is difficult to determine whether solenoid valves are in a faulty condition or not. In Fig. 13 (c), however, the proposed health indicator I_{HI} enables to precisely detect the fault conditions

with the threshold $I_{HI,th}$ of 367.0 mA, which was obtained by (15) where the mean μ_{IH} and the standard deviation σ_{IH} of new and normal valves were calculated as 358.5 mA and 2.832 mA, respectively. It can be found that health indicators I_{HI} of the faulty valve are always larger than the threshold $I_{HI,th}$, irrespective of the temperature. Therefore, the proposed physics-based method is capable of detecting faulty conditions of service braking valves in a braking system of an urban railway vehicle at any operating temperature.

VI. CONCLUSION
This study proposed a model-based fault detection method for oil burnout in a solenoid valve subjected to dynamic thermal loading. An equivalent circuit model of the valve was derived to express the explicit form of the supply current by introducing Kirchhoff's voltage law. Then, the temperature effects on the health indicators were considered by introducing the resistance-temperature relationship and Ohm's law. Finally, a new health indicator of solenoid coil burnout was devised in conjunction with the derived model.

S.-H. Jo et al.: Model-Based Fault Detection Method for Coil Burnout in Solenoid Valves Subjected to Dynamic Thermal Loading

IEEE Access

A case study of real solenoid valves used in braking systems of urban railway vehicles was presented to demonstrate the validity of the proposed method. The proposed method outperformed the existing method with the fault detection accuracy of 100%. Nonetheless, it should be noted that the accuracy was obtained with a limited number of test samples. The method does not require the installation of additional sensors. It is non-invasive. The new health indicator performed robust in real-time by compensating the effects of thermal loading fluctuations attributed by external temperature environments and Joule heating of the valve itself. Solenoid coil burnout can be monitored regardless of the operating temperature.

In the future, the proposed health indicator will be validated with additional test samples. We anticipate that the fault detection method can be used for various industrial applications. A couple of examples are (i) condition monitoring of solenoid valves in the braking systems of urban railway vehicles and (ii) inspection of defective electromagnetic actuators for product qualification.

ACKNOWLEDGMENT

REFERENCES

[1] X. Fan, Y. He, P. Cheng, and M. Fang, "Fuzzy-type fast terminal sliding-mode controller for pressure control of pilot solenoid valve in automatic transmission," *IEEE Access*, vol. 7, pp. 122342–122353, 2019.

[2] Q. Kang, Y. Li, Z. Xie, Y. Liu, and M. Zhou, "An innovative rail pressure sensor signal processing algorithm to determine the start of injection and end of injection of diesel engines with common rail injection systems," *IEEE Access*, vol. 6, pp. 64674–64687, 2018.

[3] J. I. Yoon, D. Q. Truong, and K. K. Ahn, "A generation step for an electric excavator with a control strategy and verifications of energy consumption," *Int. J. Precis. Eng. Manuf.*, vol. 14, no. 5, pp. 755–766, May 2013.

[4] J.-Y. Oh, Y.-J. Park, G.-H. Lee, and C.-S. Song, "Modeling and validation of a hydraulic systems for an AMT," *Int. J. Precis. Eng. Manuf.*, vol. 13, no. 5, pp. 701–707, May 2012.

[5] D. Kwon, M. R. Hodkiewicz, J. Fan, T. Shibutani, and M. G. Pecht, "IoT-based prognostics and systems health management for industrial applications," *IEEE Access*, vol. 4, pp. 3659–3670, 2016.

[6] H. Oh, S. Choi, K. Kim, B. D. Youn, and M. Pecht, "An empirical model to describe performance degradation for warranty abuse detection in portable electronics," *Rel. Eng. Syst. Saf.*, vol. 142, pp. 92–99, Oct. 2015.

[7] R. F. Escobar, C. M. Astorga-Zaragoza, A. C. Téllez-Anguiano, D. Juárez-Romero, J. A. Hernández, and G. V. Guerrero-Ramírez, "Sensor fault detection and isolation via high-gain observers: Application to a double-pipe heat exchanger," *ISA Trans.*, vol. 50, no. 3, pp. 480–486, Jul. 2011.

[8] J. Park, J. M. Ha, H. Oh, B. D. Youn, J.-H. Choi, and N. H. Kim, "Model-based fault diagnosis of a planetary gear: A novel approach using transmission error," *IEEE Trans. Rel.*, vol. 65, no. 4, pp. 1830–1841, Dec. 2016.

[9] K. Wang, H. Guo, A. Xu, N. J. Jameson, M. Pecht, and B. Yan, "Creating self-aware low-voltage electromagnetic coils for incipient insulation degradation monitoring for smart manufacturing," *IEEE Access*, vol. 6, pp. 69860–69868, 2018.

[10] P. Chen, T. Toyota, and Z. He, "Automated function generation of symptom parameters and application to fault diagnosis of machinery under variable operating conditions," *IEEE Trans. Syst., Man, Cybern. A, Syst. Humans*, vol. 31, no. 6, pp. 775–781, Nov. 2001.

[11] A. El Mejdoubi, A. Oukaour, H. Chaoui, H. Gualous, J. Sabor, and Y. Slamani, "State-of-charge and State-of-Health lithium-ion Batteries' diagnosis according to surface temperature variation," *IEEE Trans. Ind. Electron.*, vol. 63, no. 4, pp. 2391–2402, Apr. 2016.

[12] A. J. C. Trappey, C. V. Trappey, L. Ma, and J. C. M. Chang, "Intelligent engineering asset management system for power transformer maintenance decision supports under various operating conditions," *Comput. Ind. Eng.*, vol. 84, pp. 3–11, Jun. 2015.

[13] S. V. Angadi, R. L. Jackson, S.-Y. Choe, G. T. Flowers, J. C. Suhling, Y.-K. Chang, J.-K. Ham, and J.-I. Bae, "Reliability and life study of hydraulic solenoid valve. Part 2: Experimental study," *Eng. Failure Anal.*, vol. 16, no. 3, pp. 944–963, Apr. 2009.

[14] K. Kawashima, Y. Ishii, T. Funaki, and T. Kagawa, "Determination of flow rate characteristics of pneumatic solenoid valves using an isothermal chamber," *J. Fluids Eng.*, vol. 126, no. 2, pp. 273–279, Mar. 2004.

[15] K. Bannister, G. Giorgetti, and S. Gupta, "Wireless sensor networking for hot applications: Effects of temperature on signal strength, data collection and localization," in *Proc. 5th Workshop Embedded Netw. Sensors*, 2008, pp. 1–5.

[16] J. Al Roumy, J. Perchoux, Y. L. Lim, T. Taimre, A. D. Rakić, and T. Bosch, "Effect of injection current and temperature on signal strength in a laser diode optical feedback interferometer," *Appl. Opt.*, vol. 54, no. 2, pp. 312–318, Jan. 2015.

[17] J. Luomala and I. Hakala, "Effects of temperature and humidity on radio signal strength in outdoor wireless sensor networks," in *Proc. Federated Conf. Comput. Sci. Inf. Syst. (FedCSIS)*, Oct. 2015, pp. 1247–1255.

[18] B. Seo, S.-H. Jo, H. Oh, and B. D. Youn, "Solenoid valve diagnosis for railway braking systems with embedded sensor signals and physical interpretation," in *Proc. Annu. Conf. Prognostics Health Manage. Soc. (PHMSociety)*, 2016, pp. 1–7.

[19] H.-H. Tsai and C.-Y. Tseng, "Detecting solenoid valve deterioration in in-use electronic diesel fuel injection control systems," *Sensors*, vol. 10, no. 8, pp. 7157–7169, 2010.

[20] H. Guo, K. Wang, H. Cui, A. Xu, and J. Jiang, "A novel method of fault detection for solenoid valves based on vibration signal measurement," in *Proc. IEEE Int. Conf. Internet Things (iThings) IEEE Green Comput. Commun. (GreenCom) IEEE Cyber, Phys. Social Comput. (CPSCom) IEEE Smart Data (SmartData)*, Dec. 2016, pp. 870–873.

[21] M. Börner, H. Straky, T. Weispfenning, and R. Isermann, "Model based fault detection of vehicle suspension and hydraulic brake systems," *Mechatronics*, vol. 12, no. 8, pp. 999–1010, Oct. 2002.

[22] W. Guo, J. Cheng, Y. Tan, and Q. Liu, "Solenoid valve fault diagnosis based on genetic optimization MKSVM," in *Proc. IOP Conf. Ser., Earth Environ. Sci.*, Jul. 2018, vol. 170, Art. no. 042134.

[23] K. Mutschler, S. Dwivedi, S. Kartmann, S. Bammesberger, P. Koltay, R. Zengerle, and L. Tanguy, "Multi physics network simulation of a solenoid dispensing valve," *Mechatronics*, vol. 24, no. 3, pp. 209–221, Apr. 2014.

[24] X. Zhao, L. Li, J. Song, C. Li, and X. Gao, "Linear control of switching valve in vehicle hydraulic control unit based on sensorless solenoid position estimation," *IEEE Trans. Ind. Electron.*, vol. 63, no. 7, pp. 4073–4085, Jul. 2016.

[25] M. F. Rahman, N. C. Cheung, and K. Wee Lim, "Position estimation in solenoid actuators," *IEEE Trans. Ind. Appl.*, vol. 32, no. 3, pp. 552–559, May 1996.

[26] R. K. Wangsness, *Electromagnetic Fields*. New York, NY, USA: Wiley, 1979.

[27] D. Halliday, J. Walker, and R. Resnick, *Fundamentals of Physics*. New York, NY, USA: Wiley, 1997.

[28] H. D. Roh, H. Lee, and Y.-B. Park, "Structural health monitoring of carbon-material-reinforced polymers using electrical resistance measurement," *Int. J. Precis. Eng. Manuf.-Green Technol.*, vol. 3, no. 3, pp. 311–321, Jul. 2016.

SOO-HO JO received the B.S. degree in mechanical and aerospace engineering from Seoul National University, Seoul, South Korea, in 2016, where he is currently pursuing the Ph.D. degree in mechanical and aerospace engineering. His current research topics include fault diagnosis for a valve system and elastic metamaterial-based piezoelectric vibration energy harvesting. He was the recipient of the Bronze Prize from the KSME-SEMES Open Innovation Challenge, in 2016, the Best Paper Award from the KSME, in 2018, the Second Place Winner of the Student Paper Competition from the KSME, in 2018, the Best Paper Award from the KSNVE, in 2019, and the Second Place Winner of the PHM Society Data Challenge Competition, in 2019. He is also a recipient of the Best Paper Award from the KSME.

IEEE *Access*

S.-H. Jo *et al.*: Model-Based Fault Detection Method for Coil Burnout in Solenoid Valves Subjected to Dynamic Thermal Loading

BOSEONG SEO received the B.S. degree in mechanical and aerospace engineering from Seoul National University, Seoul, South Korea, in 2014, where he is currently pursuing the Ph.D. degree in mechanical and aerospace engineering. His research interests are in the areas of fault diagnostics and health management for a valve systems. He was a recipient of the Best Student Paper Award from ICMR, in 2015.

HYUNSEOK OH received the B.S. degree in mechanical engineering from Korea University, Seoul, South Korea, in 2004, the M.S. degree in mechanical engineering from the Korea Advanced Institute of Science and Technology, Daejeon, South Korea, in 2006, and the Ph.D. degree in mechanical engineering from the University of Maryland, College Park, MD, USA, in 2012. He is an Assistant Professor with the School of the Mechanical Engineering, Gwangju Institute of Science and Technology, Gwangju, South Korea. His research interests include prognostics and health management, and model verification and validation. He was a recipient of the A. James Clark Fellowship, in 2007, and several awards, including the IEEE PHM Data Challenge Competition Winner, in 2012, the PHM Society Data Challenge Competition Winner, in 2014 and 2015, and the ACSMO Young Scientist Award, in 2016.

BYENG D. YOUN received the B.S. degree in mechanical engineering from Inha University, Incheon, South Korea, in 1996, the M.S. degree in mechanical engineering from the Korea Advanced Institute of Science and Technology, Daejeon, South Korea, in 1998, and the Ph.D. degree in mechanical engineering from The University of Iowa, Iowa City, IA, USA, in 2001. He is a Professor with the Department of Mechanical and Aerospace Engineering, Seoul National University, Seoul, South Korea. He was the recipient of the ASME IDETC Best Paper Award, in 2001 and 2008, the ISSMO/Springer Prize for a Young Scientist, in 2005, the IEEE PHM Competition Winner, in 2014, and the PHM Society Data Challenge Competition Winner, in 2014, 2015, and 2017.

DONGKI LEE received the B.S. degree in mechanical engineering from Hanyang University, Seoul, South Korea, in 2013, and the M.S. degree in mechanical and aerospace engineering from Seoul National University, Seoul, in 2016. He is a Senior Researcher of the Productivity Research Institute, LG Electronics, Pyeongtaek, South Korea. His current research topics include prognostics and health management. He was the recipient of the PHM Society Data Challenge Competition Winner, in 2017 and 2019.

● ● ●